28th International Conference on Information Technology (IT)
Žabljak, 21 – 24 February, 2024

KF-based LOS Guidance Law for Path Following of USV: Experiments and Performance Evaluation

Žarko Zečević, Luka Martinović, Lazar Ašanin, Marco Bibuli,
Roberta Ferretti, Angelo Odetti, Simona Aracri, Massimo Caccia

***Abstract*— In this paper, we present the experimental results of the recently proposed Kalman filter-based line-of-sight (KF-based LOS) path-following algorithm tailored for Unmanned Surface Vehicles (USVs), addressing a known challenge where traditional LOS methods lack robustness against external disturbances leading to sideslip and tracking errors. A series of experiments focusing on straight-line following has been conducted, with all data systematically recorded for further analysis. The vehicle's performance is quantitatively assessed through well-known performance indices. The results demonstrate that the KF-based LOS method effectively compensates for sideslip, enabling a USV to accurately follow a straight line.**

***Index Terms*— USV, Guidance, Path Following, Line-of-Sight (LOS), Predictor-based, Sideslip Compensation**

I. Introduction

Over the past decades, researchers have shown considerable interest in unmanned surface vehicles (USVs) due to their numerous applications in marine operations [1]. Several motion control scenarios have been in focus, such as point stabilization, trajectory tracking and path following [2]. To successfully execute these motion scenarios, it is crucial to properly design the kinematic guidance law and the heading controller. Within the guidance loop, common methods encompass line-of-sight (LOS) [3]–[5] and constant bearing guidance [6]. Meanwhile, in the heading control loop, widely employed techniques include fuzzy controller [6], PID controller [7], adaptive controller [8], neural network controller [9], sliding-mode controller [10] and model-predictive controller [11].

The line-of-sight (LOS) guidance is frequently employed for path following in USVs due to its simplicity and effectiveness. The output of this guidance method is a desired yaw angle, which serves as a control input for the heading controller. The main drawback of the LOS guidance law in its traditional form is its lack of robustness to external disturbances. Namely, performance of the guidance law in its traditional form significantly deteriorates when the vehicle encounters unknown drift forces induced by environmental disturbances such as ocean currents, waves, and wind. These disturbances result in a deviation between the USV's actual orientation and its heading, referred to as sideslip, leading to increased tracking errors and overall performance deterioration [3]. Effectively addressing sideslip requires modifying the guidance law, which, in turn, necessitates knowledge of the sideslip angle. Measurement options include the use of optical correlation sensors or calculations based on surge and sway velocity measurements [12]. Nonetheless, both approaches have drawbacks, as they are either prohibitively expensive or prone to errors due to noisy measurements.

Several strategies for estimating the sideslip angle have been developed in the literature, including integral LOS [3], adaptive LOS [7], and predictor-based methods [13]. Notably, among these, predictor-based methods have proven to be the most effective in terms of performance. In a recent publication [5], the authors have introduced a novel LOS guidance law for the path following of USVs with sideslip compensation. Unlike existing predictor-based approaches that use independent adaptive gains for updating the cross-track error and sideslip angle estimations, the proposed method simultaneously estimates the sideslip angle and the cross-track error. This is achieved by treating the sideslip angle as an unknown system state and then utilizing an augmented extended Kalman filter (AEKF). The Kalman filter-based (KF-based) LOS guidance law results in faster convergence speed and improved path-following performance, as demonstrated through numerical simulations in [5].

In this paper, we present the experimental results of the KF-based LOS algorithm, which has been implemented on the SWAMP USV [14] and tested under real conditions in Genoa, Italy. The testing was conducted in cooperation with the CNR team as part of the MONUSEN project [15]. A series of experiments involving straight-line following was carried out. The results indicate that the KF-based LOS method effectively compensates for sideslip, enabling the USV to accurately follow a straight path.

II. Path-following Problem

Three reference frames are commonly employed to define the path-following problem of a USV in a 2-D plane: the earth-fixed inertial frame I, the body-fixed frame B, and the path-tangential reference frame P, as illustrated in Fig. 1.

*This paper is supported by European Union's Horizon Europe research and innovation programme under grant agreement No 101060395, Twinning project MONUSEN.

Ž. Zečević, L. Martinović and L. Ašanin are with Faculty of Electrical Engineering, University of Montenegro, Džordža Vašingtona bb, Podgorica, Montenegro, e-mails: {lukam, zarkoz}@ucg.ac.me.

M. Bibuli, R. Ferretti, S. Aracri, A. Odetti and M. Caccia are with the Institute of Marine engineering–National Research Council of Italy, Genoa 16149, Italy, e-mails: {marco.bibuli, roberta.ferretti, angelo.odetti simona.aracri, massimo.caccia}@cnr.it.

979-8-3503-6961-8/24/$31.00 ©2024 IEEE

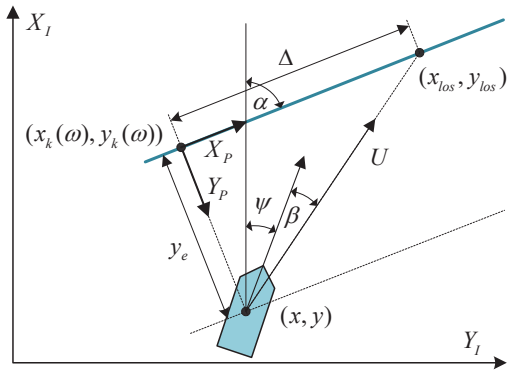

Fig. 1: LOS guidance geometry for 2-D path following.

The kinematics of an underactuated three-degrees-of-freedom USV can be represented by [5]:

$$\begin{cases} \dot{x} = u\cos\psi - v\sin\psi, \\ \dot{y} = u\sin\psi + v\cos\psi, \\ \dot{\psi} = r, \end{cases} \tag{1}$$

where (x, y) and ψ denote the position and orientation of the USV in an earth-fixed frame, whereas u, v and r denote surge, sway velocities and yaw rate in the body-fixed frame.

The reference straight-line path can be parameterized using a path variable ω:

$$\begin{cases} x_k(\omega) = x_0 + \omega\cos\alpha, \\ y_k(\omega) = y_0 + \omega\sin\alpha, \end{cases} \tag{2}$$

where (x_0, y_0) is a fixed point on the path and $\alpha = \text{atan2}(y_k'(\omega), x_k'(\omega))$ denotes the path-tangential angle, which is constant for the straight-line path following problem. The distance from the USV position (x, y) to the path, expressed in $\{P\}$ reference frame is

$$\begin{bmatrix} 0 \\ y_e \end{bmatrix} = \begin{bmatrix} \cos\alpha & -\sin\alpha \\ \sin\alpha & \cos\alpha \end{bmatrix}^T \begin{bmatrix} x - x_k(\omega^*) \\ y - y_k(\omega^*) \end{bmatrix}, \tag{3}$$

where $(x_k(\omega^*), y_k(\omega^*))$ is the normal projection of (x, y) onto the path, and y_e is the cross-track error, i.e. orthogonal distance to the desired path. Furthermore, equation (3) can be expanded into

$$\begin{cases} 0 = (x - x_k(\omega^*))\cos\alpha + (y - y_k(\omega^*))\sin\alpha \\ y_e = -(x - x_k(\omega^*))\sin\alpha + (y - y_k(\omega^*))\cos\alpha. \end{cases} \tag{4}$$

By taking the time derivative of (4) and performing some algebraic manipulations, the dynamics of the cross-track error can be expressed as [5]:

$$\dot{y}_e = U\sin(\psi - \alpha)\cos\beta + U\cos(\psi - \alpha)\sin\beta, \tag{5}$$

where $U = \sqrt{u^2 + v^2}$ is the total speed and $\beta = \text{atan2}(v, u)$ is the sideslip angle. The control objective is to ensure that $\lim_{t\to\infty} y_e(t) = 0$, which can be achieved by defining the appropriate guidance law ψ_d (the desired heading angle). In practice, PD controllers are commonly used to force the heading angle ψ to track ψ_d. The LOS guidance law has the following form:

$$\psi_d = \alpha - \arctan\frac{y_e}{\Delta}. \tag{6}$$

This guidance law ensures that the USV is oriented towards the moving target point $(x_{\text{los}}, y_{\text{los}})$ until it converges to the desired path, as depicted in Fig. 1. Here, Δ represents the look-ahead distance, determining how far ahead the target location is along the path. Although the LOS law is effective, in scenarios where the sway speed is non-zero (due to ocean currents), the cross-track error y_e will converge to a non-zero value. For this reason, modified LOS methods that involve estimation and compensation of the sideslip angle are proposed in the literature [3].

III. KF-BASED LOS GUIDANCE ALGORITHM

If we assume that the sideslip angle is small and constant, we can make the approximations $\cos(\beta) \approx 1$ and $\sin(\beta) \approx \beta$. Then, the cross-track error dynamics can be rewritten as

$$\dot{y}_e = U\sin(\psi - \alpha) + U\cos(\psi - \alpha)\beta. \tag{7}$$

Let us define the augmented state vector as $\boldsymbol{\xi} = \begin{bmatrix} y_e & \beta \end{bmatrix}^T$, where $\dot{\beta} = 0$ since a sideslip angle is constant. The dynamics of the augmented state vector can be expressed as $\dot{\boldsymbol{\xi}} = \boldsymbol{f}(\boldsymbol{\xi})$, with

$$\boldsymbol{f}(\boldsymbol{\xi}) = \begin{bmatrix} f_1 \\ f_2 \end{bmatrix} = \begin{bmatrix} U\sin(\psi - \alpha) + U\cos(\psi - \alpha)\beta \\ 0 \end{bmatrix}.$$

Furthermore, let $\hat{\boldsymbol{\xi}} = \begin{bmatrix} \hat{y}_e & \hat{\beta} \end{bmatrix}^T$ represent the estimation of $\boldsymbol{\xi}$. The objective is to design an estimator such that $(\boldsymbol{\xi} - \hat{\boldsymbol{\xi}}) \to 0$ as $t \to \infty$.

The augmented state vector can be estimated by using the Extended Kalman filter (EKF), as proposed in [5]. The update equation has the following form

$$\dot{\hat{\boldsymbol{\xi}}} = \boldsymbol{f}(\hat{\boldsymbol{\xi}}) + \mathbf{K}(y_e - \hat{y}_e), \tag{8}$$

where the time-varying Kalman gain $\mathbf{K}$ is calculated as

$$\begin{matrix} \dot{\mathbf{P}} = \mathbf{AP} + \mathbf{PA}^T - \mathbf{KCP} + \mathbf{Q} \\ \mathbf{K} = \mathbf{PC}^T\mathbf{R}^{-1} \end{matrix}. \tag{9}$$

Here, $\mathbf{P}$ represents the error covariance matrix, while $\mathbf{Q}$ and $\mathbf{R}$ are the process and noise covariance matrices, which can be used to adjust the convergence speed of the estimator.

Matrices $\mathbf{A}$ and $\mathbf{C}$ are the corresponding Jacobian matrices [5]:

$$\mathbf{A} = \begin{bmatrix} 0 & U\cos(\psi - \alpha) \\ 0 & 0 \end{bmatrix}, \ \mathbf{C} = \begin{bmatrix} 1 & 0 \end{bmatrix}. \tag{10}$$

Finally, the desired heading angle is defined as

$$\psi_d = \alpha - \arctan(\frac{1}{\Delta}y_e + \hat{\beta}). \tag{11}$$

This guidance law guarantees the convergence of the cross-track error to zero, even in the presence of constant sea currents [5].

Note that in this paper, we use an approximation of cross-track error dynamics which depends on the total speed

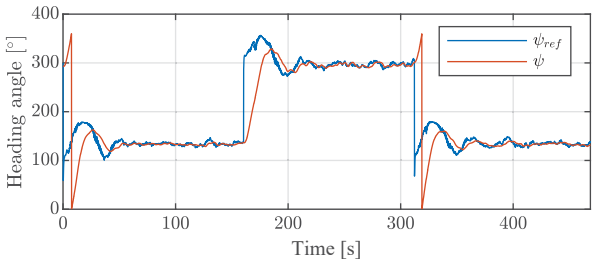

Fig. 2: Performance of the heading angle controller

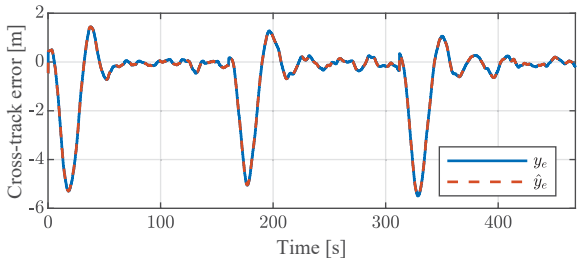

Fig. 3: Comparison of the measured and estimated cross-track error.

U, while in [5] the exact expression, dependent on u, is employed. This approach is motivated by the ease of estimating total speed from GPS data, eliminating the need for an additional sensor to measure u. As a consequence, the estimated angle remains accurate when the true sideslip angle is not large.

IV. Experimental results

The KF-based and conventional LOS guidance laws were implemented on the SWAMP USV [14], and experiments were conducted in Genoa Pra', Italy. Throughout the experiment, the USV moved approximately 130 m along the desired line ($\alpha = 60°$) at a speed of approximately 1 m/s. Subsequently, the desired angle was inverted ($\alpha = -120°$), and this process was repeated multiple times, with variations made to the algorithm parameters. The PID regulator is used as a heading controller, and its performance is shown in Fig. 2.

Figures 3 and 4 show the estimated values of the cross-track error and sideslip angle. It is evident that the KF-based LOS accurately estimates the cross-track error. This accuracy is attributed to the use of a reasonably accurate model for $\dot{y}_e$, where variations in β do not cause a significant change in y_e. On the other hand, the estimation of the sideslip angle heavily depends on the algorithm parameters. In this experiment, the covariance matrices were set to $R = 10$ and $Q = \left[\begin{smallmatrix} 100 & 0 \\ 0 & 100 \end{smallmatrix}\right]$. Due to the large value of Q, the algorithm rapidly converges to the steady-state value during the turn phase. However, for the same reason, the influence of noise on steady-state estimation is noticeable. It should be noted that the exact value of the sideslip angle is not known. For comparison purposes, we calculated $\hat{\beta}_{\text{gps}}$ as the difference between the USV direction (estimated from GPS data) and the heading angle.

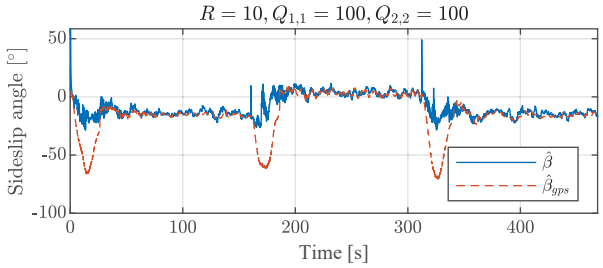

Fig. 4: Comparison of the sideslip angle estimated by KF-based LOS and from GPS data.

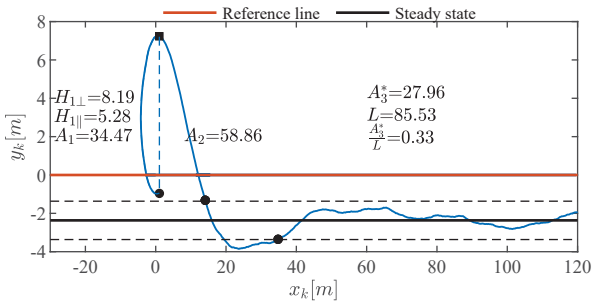

(a) Conventional LOS algorithm

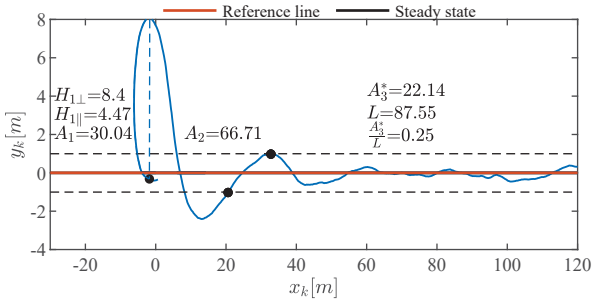

(b) KF-based LOS algorithm

Fig. 5: Comparison of the path-following performance for $\alpha = 119°$.

Figures 5 and 6 show the USV trajectory in the cases when $\alpha = 119°$ and $\alpha = -61°$. Note that in both cases, the coordinate system is set so that its abscissa coincides with the direction of the desired line. Specifically, Figs. 5a and 6a correspond to the conventional LOS algorithm, while Figs. 5b and 6b represent the KF-based LOS algorithm. To measure path-following performance, the following performance indices have been computed: 1) A_1 – area during the turning phase, 2) A_2 – area during the path approach phase, 3) A_3^* – area in the steady-state phase, 4) normalized area in the steady-state phase, 5) vertical Hausdorff distance, and horizontal Hausdorff distance. For a detailed description of performance indicators, readers are referred to [16]. In Fig. 5, the algorithms exhibit comparable performance in terms of the defined performance indices. However, in steady-state, the conventional LOS algorithm deviates by approximately 2.4 m from the desired path, while the KF-based LOS algorithm oscillates around the desired line. In the case when $\alpha = -61°$ (Fig. 6), both algorithms show smaller

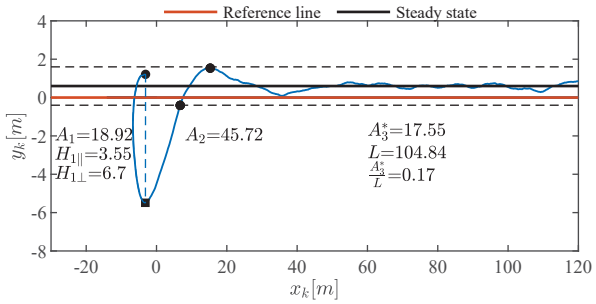

(a) Conventional LOS algorithm

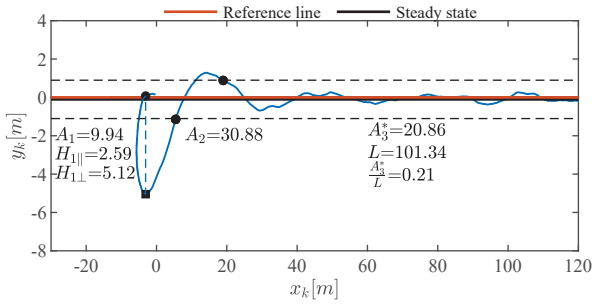

(b) KF-based LOS algorithm

Fig. 6: Comparison of the path-following performance for $\alpha = -61°$.

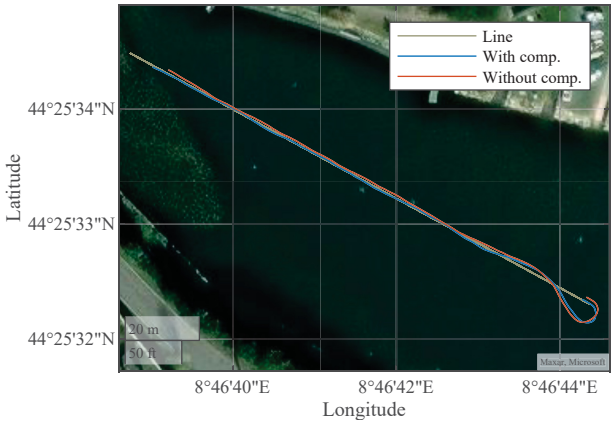

Fig. 7: Visualization of USV trajectories on Google Maps.

performance indicators during the transient phase. Moreover, the conventional LOS algorithm deviates by approximately 0.6 m from the desired path, while the KF-based LOS algorithm oscillates around the desired line. This behavior is attributed to the smaller side-slip angle in this direction, as evident in Fig. 4.

Finally, the USV trajectories and desired path are shown in Fig. 7 on Google Maps. In the KF-based LOS case, the trajectory aligns with the desired path, thus demonstrating effective sideslip compensation.

V. Conclusion

In this paper, the experimental results of the KF-based LOS algorithm, developed within the framework of the MONUSEN project, are presented. The algorithm was implemented on the SWAMP USV, and experiments were conducted in Genoa Pra', Italy. The preliminary results demonstrate that the KF-based LOS method effectively compensates for sideslip, enabling the USV to accurately follow a straight path. Future work will focus on generalizing the KF-based algorithm to accommodate generic paths and conducting experimental verification.

Acknowledgment

The authors would like to thank Giorgio Bruzzone for his support in the execution of sea trials.

References

[1] Z. Liu, Y. Zhang, X. Yu, and C. Yuan, "Unmanned surface vehicles: An overview of developments and challenges," *Annu. Rev. Control*, vol. 41, pp. 71–93, 2016.

[2] M. Bibuli, G. Bruzzone, M. Caccia, and L. Lapierre, "Path-following algorithms and experiments for an unmanned surface vehicle," *J. F. Robot.*, vol. 26, no. 8, pp. 669–688, aug 2009.

[3] W. Caharija, K. Y. Pettersen, M. Bibuli, P. Calado, E. Zereik, J. Braga, J. T. Gravdahl, A. J. Sorensen, M. Milovanovic, and G. Bruzzone, "Integral Line-of-Sight Guidance and Control of Underactuated Marine Vehicles: Theory, Simulations, and Experiments," *IEEE Trans. Control Syst. Technol.*, vol. 24, no. 5, pp. 1623–1642, 2016.

[4] N. Gu, D. Wang, Z. Peng, J. Wang, and Q. L. Han, "Advances in Line-of-Sight Guidance for Path Following of Autonomous Marine Vehicles: An Overview," *IEEE Trans. Syst. Man, Cybern. Syst.*, 2022.

[5] L. Asanin, L. Martinovic, Z. Zecevic, M. Bibuli, R. Ferretti, and M. Caccia, "Improved LOS Guidance Law for Path Following of Underactuated USV with Sideslip Compensation," *2023 27th Int. Conf. Inf. Technol. IT 2023*, 2023.

[6] Z. Peng, J. Wang, and D. Wang, "Distributed Maneuvering of Autonomous Surface Vehicles Based on Neurodynamic Optimization and Fuzzy Approximation," *IEEE Trans. Control Syst. Technol.*, vol. 26, no. 3, pp. 1083–1090, may 2018.

[7] T. I. Fossen, K. Y. Pettersen, and R. Galeazzi, "Line-of-sight path following for dubins paths with adaptive sideslip compensation of drift forces," *IEEE Trans. Control Syst. Technol.*, vol. 23, no. 2, pp. 820–827, 2015.

[8] R. Skjetne, T. I. Fossen, and P. V. Kokotović, "Adaptive maneuvering, with experiments, for a model ship in a marine control laboratory," *Automatica*, vol. 41, no. 2, pp. 289–298, feb 2005.

[9] Z. Peng, J. Wang, and D. Wang, "Distributed Containment Maneuvering of Multiple Marine Vessels via Neurodynamics-Based Output Feedback," *IEEE Trans. Ind. Electron.*, vol. 64, no. 5, pp. 3831–3839, may 2017.

[10] R. Cui, X. Zhang, and D. Cui, "Adaptive sliding-mode attitude control for autonomous underwater vehicles with input nonlinearities," *Ocean Eng.*, vol. 123, pp. 45–54, sep 2016.

[11] Z. Peng, J. Wang, and J. Wang, "Constrained Control of Autonomous Underwater Vehicles Based on Command Optimization and Disturbance Estimation," *IEEE Trans. Ind. Electron.*, vol. 66, no. 5, pp. 3627–3635, may 2019.

[12] A. Hac and M. D. Simpson, "Estimation of Vehicle Side Slip Angle and Yaw Rate," *SAE Tech. Pap.*, 2000.

[13] L. Liu, D. Wang, Z. Peng, and H. Wang, "Predictor-based LOS guidance law for path following of underactuated marine surface vehicles with sideslip compensation," *Ocean Eng.*, vol. 124, pp. 340–348, 2016.

[14] A. Odetti, G. Bruzzone, M. Altosole, M. Viviani, and M. Caccia, "SWAMP, an Autonomous Surface Vehicle expressly designed for extremely shallow waters," *Ocean Eng.*, vol. 216, p. 108205, nov 2020.

[15] S. Tomović, N. Mišković, J. Neasham, M. Caccia, Z. Zečević, F. Ferreira, L. Martinović, and I. Radusinović, "Increasing the Underwater Sensor Networks potential in Montenegro - an overview of the Horizon Europe MONUSEN project," *Ocean. 2023 - Limerick, Ocean. Limerick 2023*, 2023.

[16] E. Saggini, E. Zereik, M. Bibuli, G. Bruzzone, M. Caccia, and E. Riccomagno, "Performance Indices for Evaluation and Comparison of Unmanned Marine Vehicles' Guidance Systems," *IFAC Proc. Vol.*, vol. 47, no. 3, pp. 12 182–12 187, jan 2014.